Metallophysics and Advanced Technologies
Металофіз. новітні технол.
Metallofiz. Noveishie Tekhnol.
2021, vol. 43, No. 8, pp. 1053–1063
https://doi.org/10.15407/mfint.43.08.1053
Reprints available directly from the publisher

PACS numbers: 61.66.Dk, 61.72.S-, 64.75.-g, 68.43.Mn, 68.43.Nr, 82.30.Rs, 88.30.R-

Hydrogen Storage Properties of $Ti_{15.4}Zr_{30.2}Mn_{44}V_{5.4}Cr_5$ Alloy Produced by Induction and Arc Melting

V. A. Dekhtyarenko

G. V. Kurdyumov Institute for Metal Physics, N.A.S. of Ukraine,
36 Academician Vernadsky Blvd.,
UA-03142 Kyiv, Ukraine

On the example of the alloy $Ti_{15.4}Zr_{30.2}Mn_{44}V_{5.4}Cr_5$, the technological scheme of producing massive ingots by the technique of induction melting in open Al_2O_3 crucibles, which can be used in industry, is developed. This scheme ensures the absence of significant interaction between the crucible material and the melt, while maintaining the allowable content of aluminium impurities in the alloy, and thus achieving the required structure, phase composition, and hydrogen storage properties.

Key words: induction melting, phase composition, Laves phase, hydrogenation, dehydrogenation, hydrogen capacity.

На прикладі стопу $Ti_{15,4}Zr_{30,2}Mn_{44}V_{5,4}Cr_5$ розроблено технологічну схему одержання масивних зливків методом індукційного топлення у відкритих тиглях з Al_2O_3, яка може бути застосована у промисловості. Дана схема забезпечує відсутність суттєвої взаємодії між матеріалом тиглю та розтопом, зберігаючи допустимий вміст домішок алюмінію у стопі, завдяки чому досягається необхідна його структура, фазовий склад та водневосорбційні властивості.

Ключові слова: індукційне топлення, фазовий склад, фаза Лавеса, гідрування, дегідрування, воднева ємність.

(Received February 22, 2021; in final version, June 30, 2021)

Corresponding author: Volodymyr Anatoliyovych Dekhtyarenko
E-mail: Devova@i.ua

Citation: V. A. Dekhtyarenko, Hydrogen Storage Properties of $Ti_{15.4}Zr_{30.2}Mn_{44}V_{5.4}Cr_5$ Alloy Produced by Induction and Arc Melting, *Metallofiz. Noveishie Tekhnol.*, **43**, No. 8: 1053–1063 (2021), DOI: 10.15407/mfint.43.08.1053.

1. INTRODUCTION

Active use of hydrogen in the automotive industry requires new materials for safe storage and transportation of hydrogen in bound state in the form of metal hydrides [1, 2]. The storage of hydrogen in the form of metal hydrides is considered to be the most promising method among the existing ones [3–5].

Modern materials developed so far allow to solve specific technical problems of the hydrogen energetics (transportation or storage of hydrogen) with help of specific materials with specified properties—temperature and pressure of synthesis and decomposition of hydrides [6]. These materials primarily include magnesium [7], titanium and Ti-based b.c.c.-solid solutions [8], as well as intermetallics of various types—AB_5 (a typical example is $LaNi_5$) [9], AB (TiFe) [10] and AB_2 ($TiMn_2$) [11], and alloys based on them. According to [12], most researchers produce these materials for hydrogen accumulation by casting. However, as noted in [12], segregations inevitably occur in the cast ingots during cooling, which can adversely affect the hydrogen absorption properties. More modern methods of producing the alloys are based on hardening from the melt with high cooling rates, or on the use of powder technologies; they allow to obtain ingots and powders with higher chemical homogeneity and finer grain size as compared to traditional casting.

In [13], the hydrogen absorption characteristics of an alloy comprised of Laves phase, produced either from powders by spraying in gas or by casting followed by grinding, were compared. The authors showed that the morphology of particles depended on the parameters of their production and processing methods. The study of hydrogen absorption properties for gas-sprayed particles in comparison with those obtained by casting followed by grinding showed that at the particle size less than 50 μm the amount of absorbed hydrogen sharply decreased, and the hysteresis loop increased. The gas-sprayed alloy showed enhanced hydrogen desorption due to finer grain size.

In [14], a study of the hydrogen absorption properties of the $Ti_{0.72}Zr_{0.28}Mn_{1.6}V_{0.4}$ alloy produced by induction melting and mechanical alloying is performed. Regardless of the production method, the alloy had two-phase structure and consisted of a Laves phase of type C14 and b.c.c.-solid solution. The authors noted that the homogeneity of the elements' distribution in the phases of the alloy after induction melting is much higher, which correlated with the data obtained in [15]. The authors of [14] claimed that the best performance of the hydrogenation process is obtained at a temperature of 150°C, with hydrogen absorption by the cast alloy at a level of 2% wt., whereas in the case of mechanical alloying it is only 1.2% wt. The authors of [14] associate this significant difference with the different volume fraction

of b.c.c.-solid solution and higher content of impurities (iron and oxygen) in the alloy produced by mechanical doping.

The authors of [16] proved that changing the method of the material production can significantly increase the hydrogen capacity and improve the kinetics of the hydrogen desorption process. Comparing the hydrogen storage properties of the alloy $V_{35}(Ti, Cr)_{51}(Zr, Mn)_{14}$ produced by the techniques of sintering in the plasma of spark discharge (SPS method) and induction melting, the authors noted that the kinetic parameters of the hydrogenation process are the same, but the hydrogen capacity is different. Thus, for the alloy produced by the SPS method, the amount of absorbed hydrogen is 2.89% wt., whereas in the cast alloy it is 2.32% wt., and the amount of desorbed hydrogen at a temperature of 30°C is 60% and 34%, respectively. These significant differences in the amount of absorbed and desorbed hydrogen are explained by the fact that in the case of the SPS technique there is no diffusion redistribution of elements that form the Laves phase (manganese) in the b.c.c.-solid solution. Based on the literature data [17], the authors of [16] claim that the introduction of manganese in the Ti-based b.c.c.-solid solutions leads to a decrease in the lattice parameter and the amount of absorbed hydrogen. Summarizing all the above, we can say that in most cases changing the method of alloy production from casting to other techniques leads to a deterioration in the kinetics of sorption-desorption processes, and most importantly to a decrease of hydrogen capacity. In addition, it should be noted that even in the cases when the kinetics of sorption-desorption and hydrogen capacity are enhanced due to the changes in the route of alloy production, in practical use their application remains quite limited due to high cost of these methods and the scaling problem.

The purpose of this study is to establish the possibility of producing alloys of the Ti–Zr–Mn–V–Cr system with high hydrogen absorption ability and weight up to 1 kg by induction melting in open Al_2O_3 crucibles. This study is performed on the previously investigated composition of $Ti_{15.4}Zr_{30.2}Mn_{44}V_{5.4}Cr_5$ (in % at.) with a weigh of 30 grams produced by electric arc melting—its structure, phase composition and hydrogen storage properties are considered in detail in [18].

2. EXPERIMENTAL/THEORETICAL DETAILS

The alloy with a weight up to 1 kg is obtained by induction melting in argon atmosphere and open Al_2O_3 crucibles. Titanium sponge (TG-110), iodide Zr (99.975), electrolytic Mn (99.9), electrolytic V (99.5), electrolytic Cr (99.5) are used as starting components.

The phase composition and lattice parameters of the alloy are determined by X-ray phase analysis at a DRON-3M diffractometer.

Metallographic examinations are performed at a scanning electron

microscope VEGA3 TESCAN equipped with EDX detector XFlash610M (Bruker).

For the study of hydrogen absorption properties, a bulk cast alloy is used. The interaction of the alloy with hydrogen is studied by the Sievert's method at an IVGM-2M unit [19] at room temperature and a pressure of 0.23 MPa. The amount of absorbed hydrogen is determined by weighing with an accuracy of $1.5 \cdot 10^{-5}$ g and calculation of changing the pressure in a closed volume. The desorption of hydrogen is investigated at an automated dilatometric complex (ADC) with a mass spectrometer [20].

3. RESULTS AND DISCUSSION

At the first stage of the alloy production, it is important to develop a technological scheme for producing the ingot with satisfactory homogeneity, reduce the depletion in individual elements during the melting and minimize contamination of the ingot by impurities. To do this, it is necessary to correctly calculate initial masses of alloying elements which had different melting points and activities, to minimize the time required for melting and homogenization. To achieve this goal, several schemes of charging the elements into the crucible are tested. Initially, a scheme of charging the alloying components according to their melting point is tested, *i.e.* manganese with the lowest melting point (1246°C) at the bottom of the crucible, and the uppermost vanadium with the highest melting point (1910°C) (Fig. 1). But later it is found that the main criterion in determining the sequence of components' location is rather

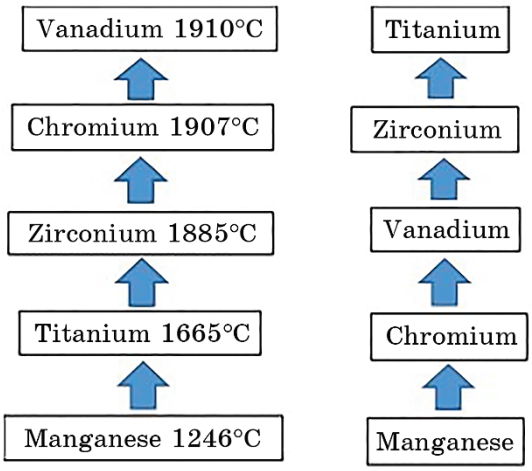

Fig. 1. The scheme of charging the components in the crucible for induction melting.

not melting points, but their mutual solubility (Fig. 1).

The following technological conditions are developed, which provide complete re-melting of the components with significantly different melting points and achieving homogeneous specified concentration of the components in the ingot (Fig. 1, right). Thus, manganese is placed on the bottom of the crucible, as it has the lowest melting point, melts first and creates a liquid bath for all other components of the charge. Although chromium has a much higher melting point than titanium and zirconium, it is placed above manganese—it has a lower density in the solid state, and when melted, it is able to rise to the top of the melt. To avoid this, vanadium with a slightly higher melting point is placed over chromium—remaining solid for a longer time, it prevented the chromium from rising. Titanium and zirconium are placed in the upper layer of the crucible charge, because they are the most active metals in comparison with other elements of the charge. They should have been in liquid state for a minimum time to minimize the time of their contact in the liquid state with the crucible. Melting the charge and the subsequent exposure of the melt under short-term RF application provided a homogeneous structure; the solidification of the alloy is carried out in the same crucible.

Given the high activity of the melt components, such as titanium, zirconium and chromium, which may react with the crucible material, it is necessary to determine whether an interaction between the melt and the crucible material, *i.e.* the reduction of aluminium from the oxide, took place. It should be noted that during the charge preparation additional (compared to the nominal composition) 4% wt. of manganese are added, because the authors of [21] studied hydrogen absorption properties of $Ti_{0.9}Zr_{0.1}Mn_{1.2}V_{0.1}$ alloy and proved that this amount of manganese can be lost due to the evaporation during melting. The chemical composition of the alloy is determined using energy-dispersion analysis EDAX (Table 1). As seen from Table 1, aluminium in the ingot is detected in small quantities, so one can conclude that no significant interaction between the crucible material and the melt has occurred.

TABLE 1. The composition of the alloy.

Composition	Elements, % at.					
	Ti	Zr	Mn	V	Cr	Al
Initial materials	15.4	30.2	44	5.4	5	–
Alloy	14.9	29.8	44.9	5.1	4.8	0.54

As seen from Table 1, the melted alloy had a slightly increased content of manganese, and the content of all other alloying elements coincided within the measurement error of ±0.3% at. with the nominal composition. The increased final manganese content can be explained by the following factors. Firstly, in the involved technological process of re-melting, the melt is exposed to high temperatures for short times. Secondly, due to the lower total amount of manganese in the charge (partial replacement by chromium) as compared to the alloy for which the calculations have been made (according to [21] for $Ti_{0.9}Zr_{0.1}Mn_{1.2}V_{0.1}$ alloy), the evaporation of manganese is lower than predicted.

It is found by scanning electron microscopy that the structure of the molten ingot, as well as the $Ti_{15.4}Zr_{30.2}Mn_{44}V_{5.4}Cr_5$ alloy obtained by the method of electric arc melting [18], comprised of coarse crystallites of the Laves phase, grain boundaries of which are decorated by b.c.c.-solid solution (Fig. 2). The obtained data indicate that the change in the technology of producing the alloy, as well as the increase in the weight of the ingot, do not critically affect the structure of the investigated material.

X-ray phase analysis confirmed the scanning electron microscopy data on that the change in the production technique, as well as the increase in the weight of the ingot, did not affect the phase composition

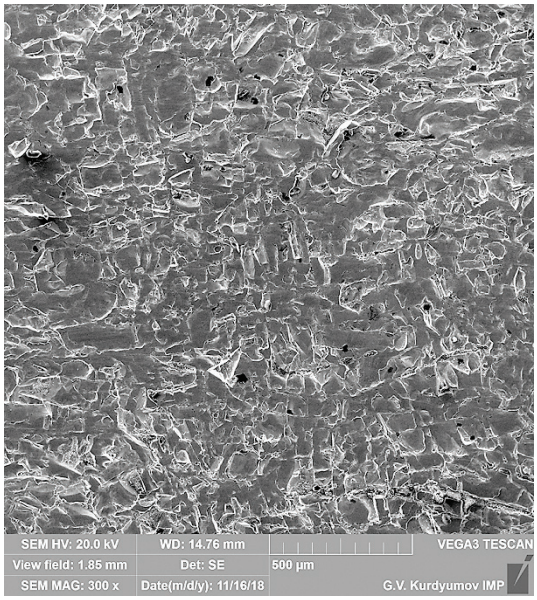

Fig. 2. Microstructure of $Ti_{15.4}Zr_{30.2}Mn_{44}V_{5.4}Cr_5$ alloy produced by induction melting.

of the alloy (Table 2). Based on the data of X-ray phase analysis and those presented in [22, 23], the volume of the elementary cell of the Laves phases and the radius of the tetrahedral internode are calculated. It is proved in [23] that, regardless of the type of crystal lattice of the Laves phase, hydrogen is localized in the tetrahedral internodes during dissolution. The authors of [22, 23] showed that the radius of the tetrahedral internode is calculated from the approximation of 'hard spheres' by the expressions Rs(C14) = 0.074475*a*, Rs(C15) = = 0.052662*a* (where *a* is the crystal lattice parameter). It is determined that regardless of the method of producing the alloy, the volume of the unit cell of the Laves phase C14 is 185 Å^3, with the radius of the tetrahedral internode 0.377 Å, and for the phase type C15 the radius is 0.378 Å.

According to the volume of the unit cell and the radius of the tetrahedral Laves phase internode for the $Ti_{15.4}Zr_{30.2}Mn_{44}V_{5.4}Cr_5$ alloy produced by different methods and with different weights, it can be seen that they coincide. Since aluminium has a much larger atomic radius (0.143 nm) than vanadium (0.124 nm), chromium (0.130 nm) and manganese (0.127 nm), its presence would increase the corresponding parameters for the alloy produced by induction melting. In addition, another proof of the lack of significant interaction between the melt and the crucible is the lack of new phases. The obtained results confirm the data of energy-dispersion analysis (EDAX) which confirmed that there is no significant interaction between the melt and the crucible in the specified technological scheme, and accordingly, there is no noticeable penetration of aluminium into the ingot.

Since the method of producing the $Ti_{15.4}Zr_{30.2}Mn_{44}V_{5.4}Cr_5$ alloy, according to scanning electron microscopy and X-ray phase analysis, did not affect the structure and phase composition, its hydrogen absorption properties are investigated at room temperature and hydrogen pressure ~0.23 MPa, as for the previous alloy [18]. The only difference

TABLE 2. The results of X-ray phase analysis of initial and hydrogenated alloys.

Alloy $Ti_{15.4}Zr_{30.2}Mn_{44}V_{5.4}Cr_5$	Parameters of crystalline lattice of phases ±0.0009 nm			
	Initial		Hydrogenated	
	C14	C15	C14	C15
Electric arc melting [18]	$a = 0.5073$ $c = 0.8334$	$a = 0.7188$	$a = 0.5489$ $c = 0.9017$	$a = 0.7776$
Induction melting	$a = 0.5070$ $c = 0.8330$	$a = 0.7191$	$a = 0.5458$ $c = 0.8966$	$a = 0.7724$

between these two experiments is the increased weight of the letter sample (up to 50 grams), while the previously studied [18] samples weighted 1–3 grams. The active absorption of hydrogen by the investigated alloy began after a few minutes of contact with a hydrogen-containing medium (the incubation period remained virtually unchanged), and lasted only five minutes with a hydrogen capacity of 2.10% wt. (H/Me ~ 1.37), whereas in the previous work [18] it is 2.12% wt. (H/Me ~ 1.38). In the alloy produced by induction melting some decrease in the amount of absorbed hydrogen occurred due to the increased manganese content. The maximum rate of hydrogen absorption is reached one minute after the start of the process, with a significant (200°C) increase in the reactor temperature (reactor weight 10 kg), which indicated the intense nature of the exothermic reaction of hydride formation. Subsequent exposure of $Ti_{15.4}Zr_{30.2}Mn_{44}V_{5.4}Cr_5$ alloy at the same hydrogenation parameters for 24 hours did not lead to the resumption of the hydrogen uptake process. Since the process of hydrogen uptake by the tested alloy is not resumed during this exposure, it can be concluded that the 50-gram sample reached the hydride state with the maximum possible hydrogen capacity in five minutes. The exposure of the hydrogenated sample at room temperature and atmospheric pressure did not lead to the beginning of the active process of hydrogen desorption, that can be considered as an evidence of its sufficient stability under these conditions.

As for the previously studied alloy [18], after the saturation by hydrogen the sample is completely destructed and transferred into the powder state due to the high rate of absorption and low hydrogenation temperature, that can be explained by the lack of time for the relaxation of stresses formed upon hydrogen dissolution. According to the data of X-ray phase analysis of the $Ti_{15.4}Zr_{30.2}Mn_{44}V_{5.4}Cr_5$, the hydrides based only on the initial phases formed in the alloy produced by induction melting upon hydrogen saturation (Table 2). According to the data of X-ray phase analysis, it can be stated that phase decomposition did not occur upon hydrogen saturation in the alloy produced by induction melting (Fig. 3). Besides, there are no changes in the structure of the metal matrix comprised of Laves phases, but only an isotropic increase in the volume of their unit cells by 20% is observed, that is in agreement with the data of [24, 25].

According to mass spectrometric studies of the gases emitted upon the heating of hydrogen-saturated $Ti_{15.4}Zr_{30.2}Mn_{44}V_{5.4}Cr_5$ alloy, regardless of the method of production, it is found that the release of hydrogen at an initial pressure of $4 \cdot 10^{-3}$ Pa started at room temperature. At room temperature, it is possible to remove no more than 3% of the absorbed hydrogen. Further hydrogen desorption is observed only upon heating (Fig. 4). Thus, at a temperature of 120°C, the maximum intensity of hydrogen desorption is reached, and at a temperature of 320°C,

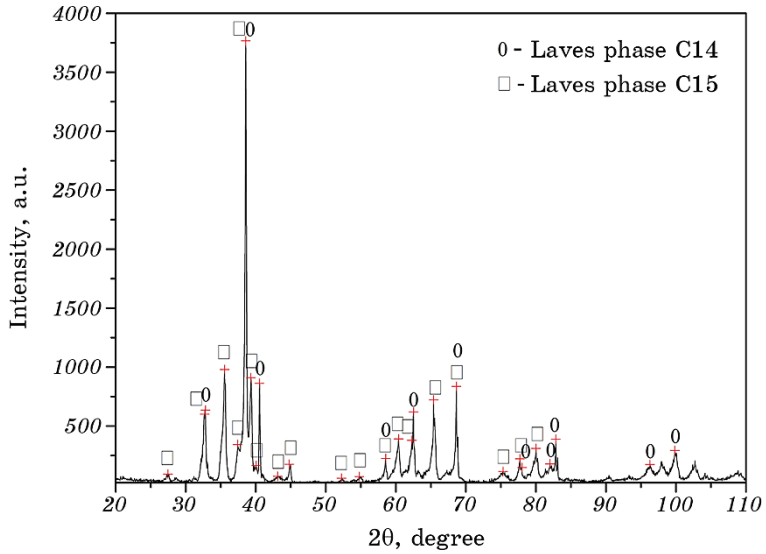

Fig. 3. Diffraction pattern of hydrogenated alloy $Ti_{15.4}Zr_{30.2}Mn_{44}V_{5.4}Cr_5$.

the desorption is completely completed. Based on the mass spectroscopy data, one can conclude that the change in the method of alloy production did not crucially affect the thermokinetic parameters of the hydrogen desorption process.

Since the hydrogen storage properties during multiple hydrogen sorption-desorption cycles are important for the hydrogen storage materials, a corresponding study is performed for the alloy $Ti_{15.4}Zr_{30.2}Mn_{44}V_{5.4}Cr_5$, regardless of the production method. The sec-

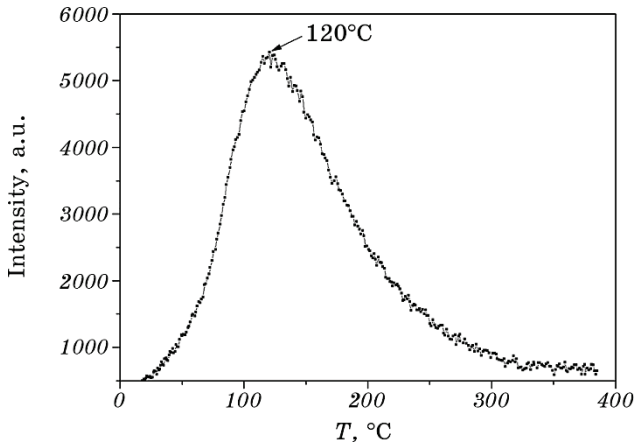

Fig. 4. Dependence of intensity of hydrogen desorption on temperature [18].

ond cycle of hydrogen sorption is performed at room temperature and an absolute pressure of 0.21 MPa. The process of hydrogen absorption started at the first seconds of contact of the sample with a hydrogen-containing medium at a high rate, while the hydrogen capacity remained unchanged. This improvement in the hydrogen sorption properties of the studied alloys in the second cycle (reduction of the incubation period from several minutes to several seconds) can be explained by the transfer of the material to the activated state by the first cycle of hydrogen sorption-desorption. Thus, this effect is caused by the destruction of bulk samples to a powder state with increasing specific surface area, as well as the partial reduction of barrier oxide scale on existing surfaces of the material as a result of its interaction with atomic hydrogen released during the first desorption.

4. CONCLUSION

A technological scheme for producing an alloy of the Ti–Zr–Mn–V–Cr system by induction melting has been developed, with no significant interaction between the crucible material and the melt and contamination of the alloy with aluminium impurities.

REFERENCES

1. G. Principi, F. Agresti, A. Maddalena, and S. L. Russo, *Energy*, **34**: 2087 (2009).
2. Bellosta von Colbe, J-R. Ares, J. Barale, M. Baricco, C. Buckley, G. Capurso, Noris Gallandat, David M. Grant, Matylda N. Guzik, Isaac Jacob, Emil H. Jensen, Torben Jensen, Julian Jepsen, Thomas Klassen, Mykhaylo V. Lototskyy, Kandavel Manickam, Amelia Montone, Julian Puszkiel, Sabrina Sartori, Drew A. Sheppard, Alastair Stuart, Gavin Walker, Colin J. Webb, Heena Yang, Volodymyr Yartys, Andreas Züttel, and Martin Dornheim, *Int. J. Hydrogen Energy*, **44**: 7780 (2019).
3. K. T. Moller, T.R. Jensen, E. Akiba, and H. W. Li, *Prog. Nat. Sci.*, **27**, 34: (2017).
4. B. Viswanathan, *Energy Sources, Hydrogen Storage* (Elsevier: 2017), p. 185.
5. S. S. Srinivasan and D. E. Demirocak, *Metal Hydrides used for Hydrogen Storage, in Nanostructured Materials for Next-Generation Energy Storage and Conversion: Hydrogen Production, Storage, and Utilization* (Eds. Y.-P. Chen, S. Bashir, and J. L. Liu (Berlin: Springer: 2017), p. 225.
6. V. N. Verbetsky and S. V. Mitrokhin, *Materialovedenie*, **1**: 48 (2009) (in Russian).
7. V. A. Yartysa, M. V. Lototskyy, E. Akiba, R. Albert, and V. E. Antonov, *Int J Hydrogen Energy*, **44**: 7809 (2019).
8. A. A. Shkola, *Metallofiz. Noveishie Tekhnol.*, **38**, No. 9: 1213 (2016) (in Ukrainian).
9. A. Narvaez, *Low Cost, Metal Hydride Based Hydrogen Storage System for*

Forklift Applications (Phase II). *US DOE Ann. Merit Rev. Meeting (June 18, 2014)* Project ST 095.
10. P. Lv, Z. Liu, A. K. Patel, X. Zhou, and J. Huot, *Metals Mater. International*, **27**: 1346 (2021).
11. M. Lototskyy, I. Tolj, Y. Klochko, M. W. Davids, D. Swanepoel, and V. Linkov, *Int. J. Hydrogen Energy*, **45**: 7958 (2020).
12. P. Pei, X. P. Song, J. Liu, G. L. Chen, X. B. Qin, and B. Y. Wang, *Int. J. Hydrogen Energy*, **34**, No 19: 8094 (2009).
13. J. H. Kim, H. Lee, K. T. Hwang, and J. S. Han, *Int. J. Hydrogen Energy*, **34**, No. 23: 9424 (2009).
14. M. Kazemipour, H. Salimijazi, A. Saidi, A. Saatchi, and A. Arefarjmand, *Int. J. Hydrogen Energy*, **39**, Iss. 24: 12784 (2014).
15. S. Suwarno, J. K. Solberg, V. A. Yartys, and B. Krogh, *J. Alloys Compd.*, **509**: S775 (2011).
16. P. Pei, X. P. Song, J. Liu, M. Zhao, and G. L. Chen, *Int. J. Hydrogen Energy*, **34**, No. 20: 8597 (2009).
17. C. Y. Seo, J. H. Kim, P. S. Lee, and J. Y. Lee, *J. Alloys Compd.*, **348**: 252 (2003).
18. V. A. Dekhtyarenko, *Metallofiz. Noveishie Tekhnol.*, **41**, No. 10: 1283 (2019).
19. G. F. Kobzenko and A. A. Shkola, *Materials Diagnostics*, **56**: 41 (1990) (in Russian).
20. O. M. Ivasishin, V. T. Cherepin, V. N. Kolesnik, and M. M. Gumenyuk, *Instrumentation and Experimental Technique*, **3**: 147 (2010) (in Russian).
21. E. A. Anikina and V. N. Verbetsky, *Int. J. Hydrogen Energy*, **36**, No. 1: 1344 (2011).
22. J. R. Johnson, *J. Less-Common Met.*, **73**: 345 (1980).
23. J. Bodega, J. F. Fernández, F. Leardini, J. R. Ares, and C. Sánchez, *J. Phys. Chem. Solids*, **72**, No. 11: 1334 (2011).
24. V. A. Dekhtyarenko, *Metallofiz. Noveishie Tekhnol.*, **37**, No. 5: 683 (2015) (in Russian).
25. S. V. Mitrokhin, T. N. Smirnova, V. A. Somenkov, V. P. Glazkov, and V. N. Verbetsky, *J. Alloys Compd.*, **356–357**: 80 (2003).